A Pathogenic Role for c-Jun Amino-Terminal Kinase Signaling in Renal Fibrosis and Tubular Cell Apoptosis

Frank Y. Ma,* Robert S. Flanc,*† Greg H. Tesch,*† Yingjie Han,*† Robert C. Atkins,*† Brydon L. Bennett,‡ Glenn C. Friedman,‡ Jui-Hsiang Fan,‡ and David J. Nikolic-Paterson*†

Department of Nephrology and †Monash University Department of Medicine, Monash Medical Centre, Clayton, Victoria, Australia; and ‡Celgene, San Diego, California

Renal fibrosis and tubular apoptosis are common mechanisms of progressive kidney disease. *In vitro* studies have implicated the c-Jun amino-terminal kinase (JNK) pathway in these processes. Both of the major JNK isoforms, JNK1 and JNK2, are expressed in the kidney, but their relative contribution to JNK signaling is unknown. This study investigated the role of JNK signaling in renal fibrosis and tubular apoptosis in the unilateral ureteral obstruction model using two different approaches: (*1*) Mice that were deficient in either JNK1 or JNK2 and (2) a specific inhibitor of all JNK isoforms, CC-401. Western blotting and immunostaining identified a marked increase in JNK signaling in the obstructed kidney, with substantial redundancy between JNK1 and JNK2 isoforms. Administration of CC-401 blocked JNK signaling in the rat obstructed kidney and significantly inhibited renal fibrosis in terms of interstitial myofibroblast accumulation and collagen IV deposition. This effect was attributed to suppression of gene transcription for the profibrotic molecules TGF-β1 and connective tissue growth factor. CC-401 treatment also significantly reduced tubular apoptosis in the obstructed kidney. Genetic deletion of JNK1 or JNK2 did not protect mice from renal fibrosis in the unilateral ureteral obstruction model, but JNK1 deletion did result in a significant reduction in tubular cell apoptosis. In conclusion, this is the first study to demonstrate that JNK signaling plays a pathogenic role in renal fibrosis and tubular apoptosis. Furthermore, JNK1 plays a nonredundant role in tubular cell apoptosis. These studies identify the JNK pathway as a potential therapeutic target in progressive kidney disease.

J Am Soc Nephrol 18: 472–484, 2007. doi: 10.1681/ASN.2006060604

Progressive forms of kidney disease feature common pathologic processes such as fibrosis and the loss of intrinsic renal cells *via* apoptosis. These mechanisms operate irrespective of the nature of the initial renal insult and therefore are potential targets for therapeutic intervention. The c-Jun amino-terminal kinase (JNK) pathway has been implicated in tubular cell apoptosis on the basis of *in vitro* studies, but the functional role of JNK signaling in renal fibrosis has not been examined.

A variety of cellular stresses, such as stretch, reactive oxygen species, inflammatory cytokines, and osmotic stress, can induce a cascade of signaling events, leading to dual phosphorylation of the Thr-X-Tyr activation motif of JNK (1,2). The active (phosphorylated) form of JNK then can translocate to the nucleus and phosphorylate specific target proteins to induce a variety of cellular responses, including inflammation and apoptosis. A unique JNK target is the phosphorylation of Ser63 and Ser73 in the NH_2-terminal domain of c-Jun (3–6), which can be used as a surrogate marker of JNK activity.

Three members of the JNK family have been described in mammalian cells (1,2). JNK1 and JNK2 isoforms are widely expressed in most tissues, including the kidney, but JNK3 is restricted to the nervous system. Mice that are deficient in *Jnk1* or *Jnk2* are viable, but the double-gene knockout is fetal lethal. Transcription of each JNK gene can give rise to multiple 54- and 46-kD proteins through alternative mRNA splicing (1,2).

A proapoptotic role for JNK signaling has been demonstrated in a range of different cell types *in vitro*, although some studies have shown that JNK also can exert an antiapoptotic effect under certain circumstances (7–9). *In vivo* studies have shown that excitotoxicity-induced neuron apoptosis largely depends on JNK3 (10), whereas the use of a specific JNK inhibitor reduced hepatocyte apoptosis in liver ischemia/reperfusion injury (11,12). A role for the JNK pathway in the inflammatory response is evident from *in vitro* studies in which blockade of JNK signaling inhibits LPS-induced cytokine and nitric oxide production by macrophages (13). These data are supported by *in vivo* studies in which joint inflammation and erosion in rat adjuvant-induced arthritis was suppressed by administration of a JNK inhibitor drug (14). Furthermore, gene knockout studies have shown that JNK1 is important in the primary immune response in which naïve T cells differentiate into Th1 cells (15,16), whereas JNK2 has been implicated in the differentiation of $CD4^+$ T cells into Th1 responders (17).

In contrast to inflammation and apoptosis, little is known of JNK in tissue fibrosis. *In vitro* studies suggest a role for JNK signaling in TGF-β1 induced fibronectin production in fibro-

Received June 12, 2006. Accepted November 24, 2006.

Published online ahead of print. Publication date available at www.jasn.org.

Address correspondence to: Dr. David J. Nikolic-Paterson, Department of Nephrology, Monash Medical Centre, 246 Clayton Road, Clayton, Victoria 3168, Australia. Phone: +61-3-9594;3535; Fax: +61-3-9594-6530; E-mail: david.nikolic-paterson@med.monash.edu.au

ISSN: 1046-6673/1802-0472

blasts and in TGF-β1 induced connective tissue growth factor (CTGF) production (18,19). However, a role for JNK signaling in tissue fibrosis has yet to be demonstrated clearly.

JNK activation has been described in a variety of experimental kidney diseases (20–22), but the functional role of this pathway has not been determined in any model of kidney disease to date. We examined the pathologic role of JNK in fibrosis and apoptosis in the obstructed kidney. Unilateral ureteral obstruction (UUO) was selected because there is rapid development of renal fibrosis plus tubular apoptosis in this model. The development of fibrosis in this model depends on the profibrotic growth factors TGF-β1 and CTGF (23–25). Another important aspect of this disease model is that renal fibrosis and apoptosis are driven by irreversible mechanical stretch and are independent of the adaptive immune response (26). Two approaches were used to block JNK activity. First, *Jnk1* and *Jnk2* gene–deficient mice were examined in the mouse UUO model. Second, a specific JNK inhibitor, CC-401, was administered in the rat UUO model.

Materials and Methods

Antibodies

The following rabbit antibodies were obtained from Cell Signaling (San Diego, CA): JNK2 (preferentially detects JNK2 over JNK1), phospho-JNK (Tyr183/Tyr185), c-Jun, phospho-c-Jun (Ser63), phospho-c-Jun (Ser73), phospho-p44/42 MAPK (Thr202/Tyr204), and cleaved caspase-3. Other antibodies used were rabbit anti-JNK1/2 and goat anti–glyceraldehyde-3-phosphate dehydrogenase (Santa Cruz Biotechnology, Santa Cruz, CA); mouse anti–α smooth muscle actin (α-SMA; 1A4; (Sigma-Aldrich, Castle Hill, NSW, Australia); goat anti-collagen IV (Southern Biotechnology Associates, Birmingham, AL); rabbit anti–aquaporin 2 (anti-AQP2; Calbiochem, San Diego, CA) as a marker of collecting ducts; mouse anti-CD68, which recognizes rat macrophages (ED1), and rat anti-mouse macrophages (F4/80; Serotec, Oxford, UK); and mouse anti-bromodeoxyuridine (Dako, Glostrup, Denmark). Other antibodies included biotinylated goat anti-rabbit IgG, biotinylated rabbit anti-goat IgG, and streptavidin-conjugated horseradish peroxidase (all from Zymed-Invitrogen, Carlsbad, CA) and horseradish peroxidase–conjugated goat anti-mouse IgG and mouse peroxidase–conjugated antiperoxidase complexes (PAP; Dako).

Animals

Breeding pairs of *MAPK8* (*Jnk1*+/−) and *MAPK9* (*Jnk2*−/−) gene knockout mice on the C57BL/6J background were imported from Jackson Laboratories (Bar Harbor, ME) and bred in-house. Wild-type C57BL/6J mice and Sprague-Dawley rats were obtained from Monash Animal Services (Clayton, VIC, Australia). All animal experimentation was approved by the Monash Medical Centre Animal Ethics Committee.

Mouse Model of Renal Fibrosis

UUO surgery was performed on groups of eight female mice (22 to 25 g) of each genotype. Briefly, mice were anesthetized using ketamine/xylazine; a midline incision made; and the left ureter was exposed, tied at two points, and then cut between these ties. Animals were killed 7 d after surgery, and tissue was removed for analysis. All animals were given 50 mg/kg bromodeoxyuridine (BrdU) by intraperitoneal injection 3 h before being killed to label dividing cells.

Western Blot Analysis

A quarter kidney was homogenized in 0.5 ml of RIPA lysis buffer then centrifuged to remove debris, and the supernatant stored at −80°C. Samples were separated by SDS-PAGE; electroblotted onto nitrocellulose membranes that were incubated with Blocking Buffer (LiCor Biosciences, Lincoln, NE) before incubation with primary antibody overnight at 4°C, washing, and then incubation with Alexa Fluor 680 goat anti-rabbit IgG (Molecular Probes, Eugene, OR) for 30 min; and analyzed by the Odyssey infrared imaging system (LiCor Biosciences). Blots were reprobed for glyceraldehyde-3-phosphate dehydrogenase as a loading control. Results were quantified using the Gel-Pro Analyzer program (Media Cybernetics, Silver Spring, MD).

CC-401

The specific JNK inhibitor CC-401 was synthesized by Celgene (11,12). CC-401 is a potent inhibitor of all three forms of JNK (Ki of 25 to 50 nM) and has at least 40-fold selectivity for JNK compared with other related kinases, including p38, extracellular signal–regulated kinase (ERK), inhibitor of κB kinase (IKK2), protein kinase C, Lck, zeta-associated protein of 70 kDa (ZAP70). In cell-based assays, 1 to 5 μmol/L CC-401 provides specific JNK inhibition. CC-401 is prepared in a sodium citrate vehicle and administered to rats by twice-daily gavage at 100 mg/kg. Peak serum levels (approximately 1 μmol/L) occur 3 to 5 h after gavage. Serum levels of CC-401 were analyzed by HPLC.

CC-401 Treatment of Rat Renal Fibrosis

Groups of 10 to 14 Sprague-Dawley rats (150 to 180 g) underwent UUO surgery as described for mice above. Rats received CC-401, vehicle alone, or no treatment beginning 3 h before UUO surgery and continuing twice daily until being killed on day 7. A group of normal rats also were examined. Animals were given 50 mg/kg BrdU by intraperitoneal injection 3 h before being killed to label dividing cells.

Renal Histology

Paraffin sections (2 μm) of methylcarn-fixed tissue were stained using periodic acid-Schiff and hematoxylin. Renal interstitial area in the UUO model was assessed by point counting of the entire cortex using ×250 fields. All scoring was performed on blinded slides.

Immunohistochemistry

Immunoperoxidase staining for phosphorylated JNK (p-JNK), c-Jun, p-c-Jun Ser63, p-c-Jun Ser73, p-ERK, and AQP2 was performed on 4-μm sections of formalin-fixed tissue using antigen retrieval (microwave oven heating in 0.1 M sodium citrate [pH 6.0] for 10 min) followed by a three-layer avidin-biotin peroxidase complex (ABC) staining method (27). Immunoperoxidase staining for cleaved caspase-3 and ED1$^+$ macrophages was performed on formalin-fixed tissue sections without antigen retrieval and using a three-layer PAP staining method. Immunoperoxidase staining for α-SMA used a three-layer PAP method on methylcarn-fixed tissue, and immunostaining for collagen IV used frozen sections with the avidin-biotin peroxidase complex method. Two-color immunostaining for AQP2 and p-JNK used formalin-fixed tissue sections as described previously (27).

Quantification of Immunostaining

The interstitial area of α-SMA and collagen IV immunostaining was quantified in ×250 power fields that covered at least 90% of the cortex by image analysis using Image-Pro software (Media Cybernetics). Large blood vessels were excluded from the analysis.

The number of interstitial ED1$^+$ macrophages was counted in the entire cortex using high-power fields (×400). In addition, the number of

tubular epithelial cells and interstitial cells that stained for cleaved caspase-3 was scored in the entire cortex under high power. All scoring was performed on blinded slides.

Real-Time Reverse Transcriptase–PCR

Total RNA was extracted from whole kidney samples using the RiboPure reagent (Ambion, Austin, TX) and reverse-transcribed using the Superscript First-Strand Synthesis kit (Invitrogen, Carlsbad, CA) with random primers. Real-time PCR was performed on Rotor-Gene 3000 system (Corbett Research, Sydney, Australia) with thermal cycling conditions of 37°C for 10 min and 95°C for 5 min, followed by 50 cycles of 95°C for 15 s, 60°C for 20 s, and 68°C for 20 s. The primer pairs and FAM-labeled minor groove binder probes used were as follows: TGF-β1 forward GGA CAC ACA GTA CAG CAA, reverse GAC CCA CGT AGT AGA CGA T and probe ACA ACC AAC ACA ACC C); CTGF forward CGT TTG TGC CTA TTG TTC TTG T, reverse GAT CCA TTG CTT TAC CGT CTA C, and probe CAA ACT CCA AAC ACC A); and collagen IV forward GGC GGT GCA CAG TCA GAC CAT, reverse GGA ATA GCC AAT CCA CAG TGA, and probe CAG TGC CCC AAC GGT). The relative amount of mRNA was calculated using comparative Ct ($\Delta\Delta$Ct) method. All specific amplicons were normalized against 18S RNA, which was amplified in the same reaction as an internal control using commercial assay reagents (Applied Biosystems, Scoresby, Australia).

Tubular Cell Culture

Human HK-2 proximal tubular epithelial cells (American Type Culture Collection, Manassas, VA) were cultured in DMEM/F12 media (Sigma-Aldrich) supplemented with 10% FCS, 10 ng/ml EGF (Sigma-Aldrich), and 10 μg/ml bovine pituitary extract (Life Technologies Invitrogen, Carlsbad, CA). For Western blot studies, cells were seeded into six-well plates and allowed to adhere overnight, and medium was changed to DMEM/F12 supplemented with only 0.5% FCS for 24 h, by which time cells were confluent. CC-401 was prepared in citric acid (pH 5.5) and added to the confluent cells 1 h before the addition of 300 mM sorbitol, and cells were harvested 30 min later using urea-RIPA buffer as described previously. Three experiments were performed, each with two replicates per condition. For ELISA experiments, HK-2 cells were seeded into 24-well plates, allowed to adhere overnight, cultured in DMEM/F12 with 0.5% FCS for 24 h, and then incubated with CC-401 or vehicle for 60 min before stimulation with 1 μM angiotensin II (AngII; Sigma-Aldrich). Supernatants were harvested 48 h later and assayed for TGF-β1 content using a commercial ELISA kit (Promega, Annandale, NSW, Australia). Three experiments were performed, each using six replicates per condition.

Statistical Analyses

Data are presented as means ± 1 SD. Analysis between groups of animals was performed by ANOVA using Tukey post test for multiple comparisons (GraphPad 4.0 Software, San Diego, CA).

Results

JNK Activation in Normal and Obstructed Mouse Kidney

Western blotting with an antibody that recognizes both JNK1 and JNK2 (JNK1/2) shows abundant JNK1/2 protein in the normal kidney from wild-type, *Jnk1*−/−, and *Jnk2*−/− mice (Figure 1A). An anti-JNK2 antibody, which preferentially recognizes JNK2 over JNK1, detects strong JNK bands in wild-type and *Jnk1*−/− mice, which largely are absent in *Jnk2*−/− mice (Figure 1B). The high level of JNK1 and JNK2 expression

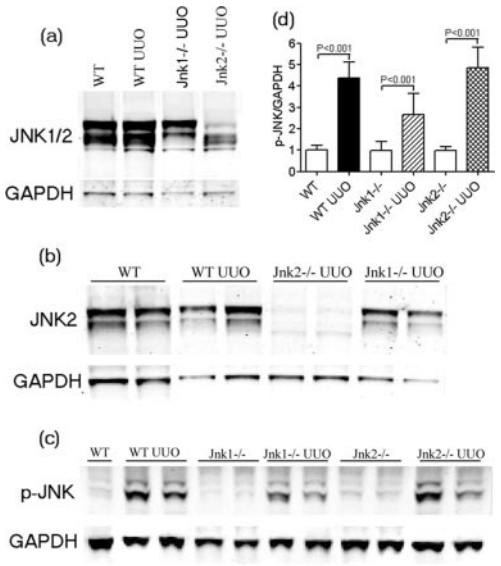

Figure 1. Detection of c-Jun amino-terminal kinase (JNK) phosphorylation in wild-type (WT), *Jnk1*−/−, and *Jnk2*−/− mice by Western blotting of whole-kidney lysates. (A) Detection of total JNK1 and JNK2 (JNK1/2) in WT normal mice and in WT, *Jnk1*−/−, and *Jnk2*−/− mice with 7 d of unilateral ureteric obstruction (UUO). (B) Detection of JNK2 in the same groups as in A. (C) Detection of phosphorylated-JNK (p-JNK) in normal and UUO kidney from WT, *Jnk1*−/−, and *Jnk2*−/− mice. Blots also were probed for glyceraldehyde-3-phosphate dehydrogenase as a loading control. (D) Graph summarizing quantification of Western blotting results for p-JNK. Data are means ± SD for groups of eight mice with statistical analysis by ANOVA.

is not affected after 7 d of UUO. A weak signal for p-JNK is evident in normal kidney from wild-type, *Jnk1*−/−, and *Jnk2*−/− mice. UUO results in a three- to five-fold increase in JNK phosphorylation in all three genotypes, indicating substantial redundancy in signaling through JNK1 and JNK2 in the obstructed kidney (Figure 1, C and D), although the level of JNK phosphorylation in the obstructed kidney of *Jnk1*−/− mice was significantly less than that seen in wild-type and *Jnk2*−/− mice ($P < 0.001$ for both).

Immunostaining localized p-JNK to collecting ducts in the cortex and the medulla and to some parietal epithelial cells in normal kidney (Figure 2A), with occasional glomerular cells also stained. Double immunolabeling confirmed co-localization of p-JNK staining in AQP2-stained collecting ducts (data not shown). This staining pattern for p-JNK was not altered in the kidney of normal *Jnk1*−/− or *Jnk2*−/− mice (data not shown). UUO induced a marked increase in JNK phosphorylation with p-JNK staining prominent in dilated, atrophic tubules as well as in morphologically normal tubules and in interstitial cells (Figure 2D). A similar increase in p-JNK staining is seen in the obstructed kidney in *Jnk1*−/− and *Jnk2*−/− mice (Figure 2, G and J), indicating that both JNK isoforms are activated in the damaged kidney.

We examined JNK activity by immunostaining for phosphorylation of c-Jun at Ser63, considered a JNK-specific target (3–5). c-Jun protein largely is absent from normal kidney (Figure 2B),

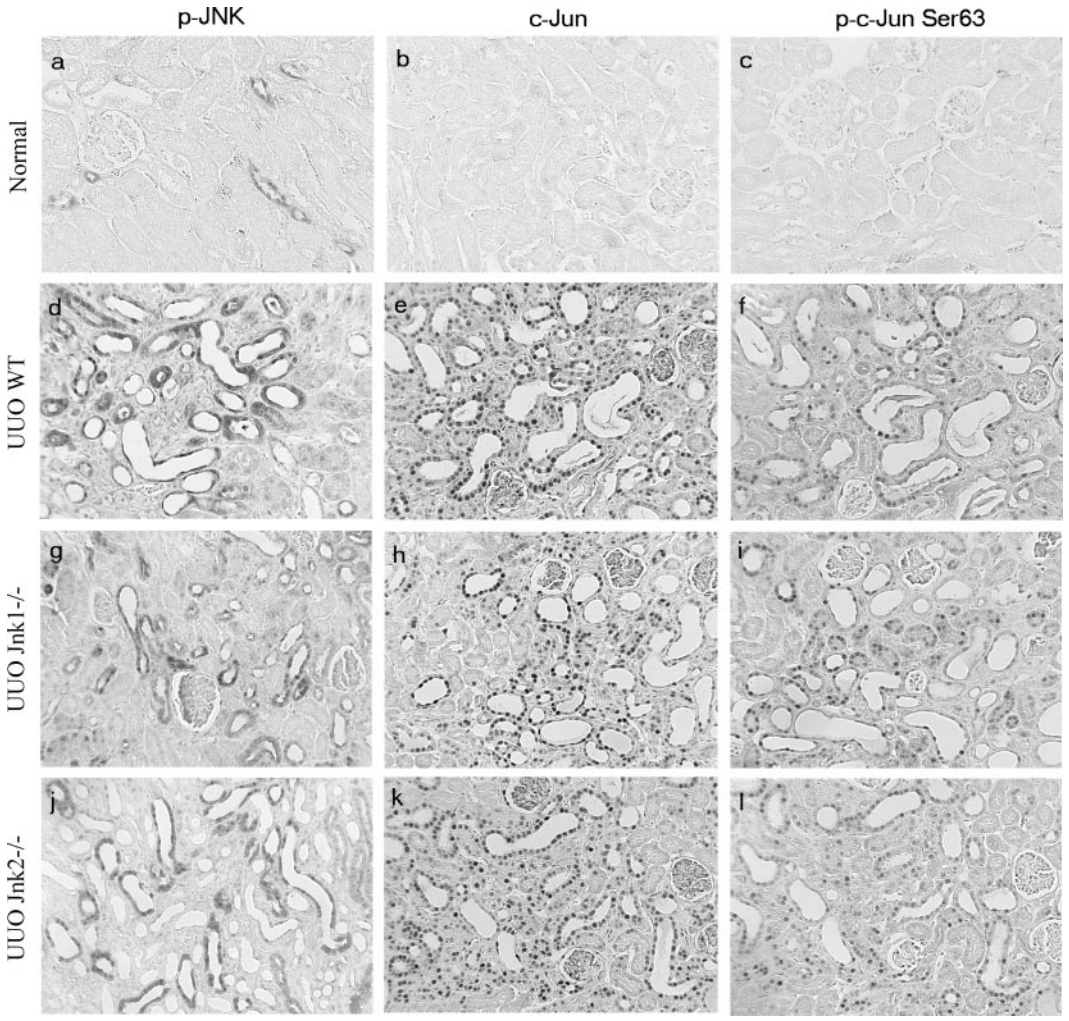

Figure 2. Detection of JNK activation by immunoperoxidase staining in mouse UUO. (A) Immunostaining for phosphorylated JNK (p-JNK) in normal mouse kidney shows a positive signal in the cytoplasm and nucleus of collecting duct cells in the renal cortex. No signal is apparent for c-Jun (B) or p-c-Jun Ser63 (C) in normal mouse kidney. (D) A marked increase in p-JNK immunostaining is apparent in UUO in WT mice, with staining of 30 to 50% of cortical tubules, many of which show marked dilation. (E) There is a dramatic induction of c-Jun in WT UUO kidney with many tubular cells showing strong nuclear staining, including dilated tubules, with a similar distribution to that of p-JNK staining. (F) Serial section to E shows immunostaining for p-c-Jun Ser63 that exhibits a pattern of nuclear staining that correlates very closely to that of total c-Jun, except that fewer cells are stained. UUO in *Jnk1*−/− mice induced a very similar increase in p-JNK (G), c-Jun (H), and p-c-Jun Ser63 (I) immunostaining as that observed in UUO in WT mice. Similarly, UUO in *Jnk2*−/− induced a very similar increase in p-JNK (J), c-Jun (K), and p-c-Jun Ser63 (L) immunostaining as that observed in UUO in WT mice. Magnification, ×250.

but it is prominent in both damaged and intact tubules and in interstitial cells in the obstructed kidney (Figure 2E). Lack of either *Jnk1* or *Jnk2* did not affect the induction of c-Jun in the obstructed kidney (Figure 2, H and K). Although absent in normal kidney, phosphorylation of c-Jun at Ser63 was evident in dilated, atrophic tubules as well as in intact tubules and interstitial cells in the obstructed kidney (Figure 2, C and F) in a pattern that corresponds exactly with total c-Jun expression and is similar to that of JNK phosphorylation. The pattern of immunostaining for p-c-Jun Ser63 in the obstructed kidney of *Jnk1*−/− and *Jnk2*−/− mice was not different from that seen in wild-type mice (Figure 2, I and L), again demonstrating redundancy in signaling. As an additional control, nuclear staining for phosphorylation of c-Jun at Ser73 (another specific JNK target) followed the same pattern as that of phosphorylation of c-Jun at Ser63 (data not shown).

Renal Fibrosis and Apoptosis in the Obstructed Mouse Kidney

UUO in wild-type mice results in marked tubular dilation and an increase in interstitial volume with development of renal fibrosis in terms of interstitial accumulation of α-SMA$^+$ myofibroblasts and deposition of collagen IV (Figure 3, A through C). *Jnk1*−/− mice showed a minor reduction in interstitial volume and in the accumulation of α-SMA$^+$ myofibroblasts, but there was no change in the deposition of collagen IV

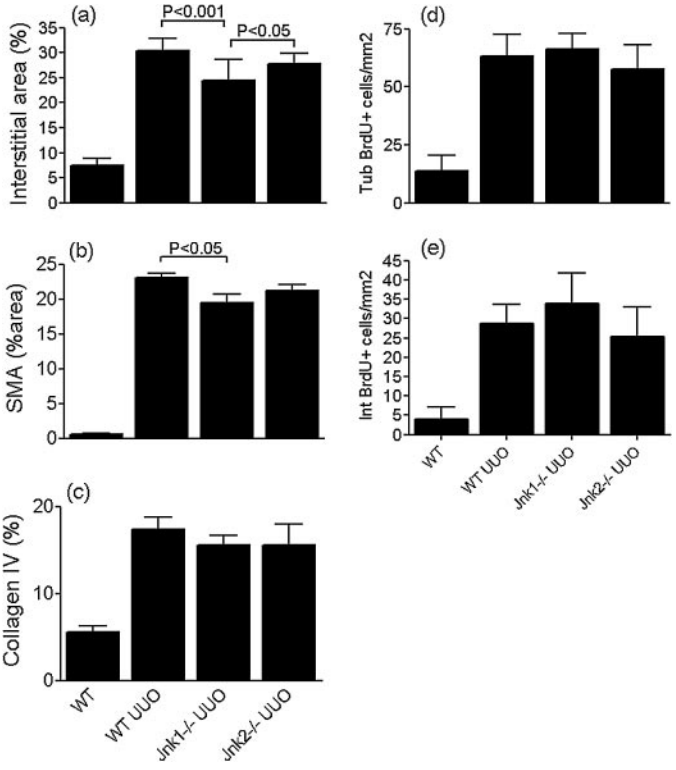

Figure 3. Quantification of renal fibrosis and apoptosis in mouse UUO. UUO was induced in groups of WT, *Jnk1*−/−, and *Jnk2*−/− mice and compared with normal mice for interstitial area (A), area of α-smooth muscle actin (α-SMA) immunostaining (B), area of collagen IV immunostaining (C), and the number of proliferating tubular cells (D) and interstitial cells (E), on the basis of immunostaining for bromodeoxyuridine (BrdU) incorporation. Data are means ± SD for groups of eight mice with statistical analysis by ANOVA.

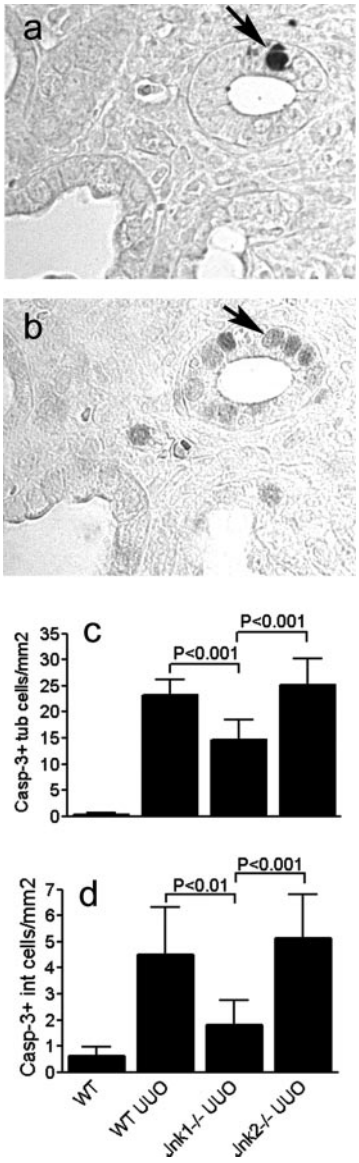

Figure 4. Apoptosis in mouse UUO. UUO was induced in groups of WT, *Jnk1*−/−, and *Jnk2*−/− mice, and apoptotic cells were identified by immunostaining for cleaved caspase-3. Immunostaining of serial sections of WT UUO kidney shows a cleaved caspase-3$^+$ tubular cell (A, arrow), and the same cell is stained for p-c-Jun Ser63 (B, arrow). Graphs show quantification of the number of tubular cells (C) and interstitial cells (D), stained for cleaved caspase-3. Data are means ± SD for groups of eight mice with statistical analysis by ANOVA (C and D). Magnification, ×400.

after UUO (Figure 3, A through C). *Jnk2*−/− mice showed no protection from renal fibrosis.

Apoptosis in the obstructed kidney was identified by immunostaining for cleaved caspase-3. Although immunostaining of serial sections was able to identify JNK activation (p-c-Jun Ser63 staining) in some apoptotic cells (Figure 4, A and B), most apoptotic cells did not show JNK activation. *Jnk1*−/− mice showed significant protection from apoptosis of tubular epithelial cells and interstitial cells in the UUO model, whereas *Jnk2*−/− mice were not protected (Figure 4, C and D). Finally, substantial proliferation of both tubular and interstitial cells was evident in the wild-type obstructed kidney on the basis of immunostaining for BrdU-labeled cells, and this was not altered in *Jnk1*−/− or *Jnk2*−/− UUO mice (Figure 3, D and E).

JNK Blockade Suppresses Renal Fibrosis in the Obstructed Rat Kidney

Given the redundancy in JNK1 and JNK2 signaling that was observed in the obstructed mouse kidney, we sought to block the activity of both JNK isoforms. For this purpose, we used CC-401, a small molecule that is a specific inhibitor of all three JNK isoforms (11,12). CC-401 competitively binds the ATP binding site in JNK, resulting in inhibition of the phosphorylation of the N-terminal activation domain of the transcription factor c-Jun. The specificity of this inhibitor was tested *in vitro* using osmotic stress of the HK-2 human tubular epithelial cell line. CC-401 inhibited sorbitol-induced phosphorylation of c-Jun in a dosage-dependent manner (Figure 5). However, CC-401 did not prevent sorbitol-induced phosphorylation of JNK, p38, or ERK. *In vivo* studies using CC-401 were performed in the rat UUO model because of the poor pharmacokinetics of

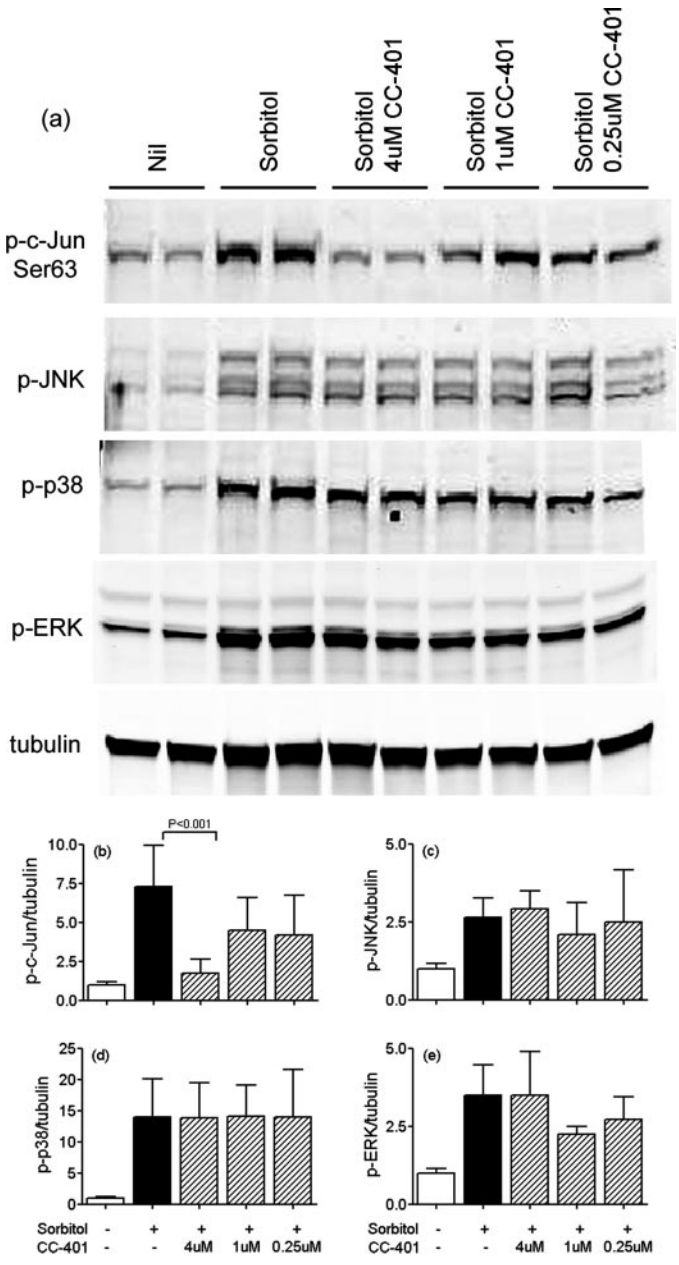

Figure 5. CC-401 inhibits c-Jun phosphorylation in tubular epithelial cells. Human HK-2 tubular epithelial cells were incubated with various concentrations of CC-401 and then given an osmotic shock with 300 mM sorbitol for 30 min. (A) Cell lysates were examined by Western blotting for p-c-Jun Ser63, p-JNK, p-p38, and phosphorylated extracellular signal–regulated kinase (p-ERK), and blots were reprobed for tubulin. (B through E) Graphs of the various phosphorylated proteins relative to tubulin showing pooled data from three independent experiments. Data are means ± SD with statistical analysis by ANOVA.

CC-401 in the mouse. However, the pathologic changes and mechanisms of fibrosis in the obstructed kidney are very similar in the rat and the mouse.

Ureter ligation of the rat kidney induced a marked increase in p-JNK staining with the induction of c-Jun expression and detection of phosphorylation of c-Jun on Ser63 in a pattern very similar to that in the obstructed mouse kidney (Figure 6). Administration of CC-401 partially reduced JNK phosphorylation (Figure 6I), and there was an almost complete absence of phosphorylation of c-Jun at Ser63 in the obstructed kidney (Figure 6J). As an additional control, we performed immunostaining with an antibody against p-c-Jun Ser73, which is another JNK-specific target, although this antibody also recognizes phosphorylation of JunD at Ser100. Normal rat kidney shows positive staining with the antibody against p-c-Jun Ser73 in the luminal surface of collecting duct cells (Figure 6C). Because c-Jun is absent from tubular cells in normal kidney, this staining presumably reflects phosphorylation of JunD at Ser100 given that JunD is expressed constitutively in normal kidney (28). In the ligated kidney, nuclear staining for p-c-Jun Ser73 followed a virtually identical pattern to that seen for p-c-Jun Ser63 (Figure 6G). The nuclear p-c-Jun Ser73 staining was abrogated by CC-401 treatment, although weak luminal staining of dilated tubules was apparent. This luminal staining presumably reflects p-JunD Ser100 because it is known that JunD is upregulated in the injured kidney (28). We also examined activation of ERK because this kinase is related closely to JNK and ERK can phosphorylate JunD at Ser100 (5). Immunostaining showed p-ERK in collecting ducts in normal rat kidney, and there was marked p-ERK staining in damaged and normal tubules and in interstitial cells in the obstructed kidney, which was unaltered by CC-401 treatment (Figure 6, D, H, and L). Western blot analysis of whole-kidney tissue confirmed a substantial increase in the phosphorylation of JNK, ERK, and p38 kinases in the rat UUO kidney (all $P < 0.05$ *versus* normal). However, no significant differences were seen in phosphorylation of JNK, ERK, or p38 kinases between the no-treatment, vehicle-treated, and CC-401–treated UUO groups (Figure 7). Animals were killed 2 h after the last drug administration, at which time serum CC-401 levels were 1.65 ± 1.17 μM, indicating that peak blood levels were in the target range in which the drug is highly specific for inhibiting JNK activity.

UUO in untreated or vehicle-treated rats resulted in marked tubular dilation with an increase in interstitial volume as a result, in part, of interstitial accumulation of α-SMA$^+$ myofibroblasts and deposition of collagen IV (Figure 8). A significant increase in kidney mRNA levels for collagen IV and for the profibrotic growth factors TGF-β1 and CTGF was evident in untreated and vehicle-treated UUO (Figure 9). Despite ongoing ureter ligation that causes tubular dilation, CC-401 treatment significantly reduced interstitial volume, α-SMA$^+$ myofibroblast accumulation, and the deposition of collagen IV (Figure 8). These effects were associated with a partial reduction in renal TGF-β1 and collagen IV mRNA levels and normalization of renal CTGF mRNA levels (Figure 9).

To investigate whether JNK blockade directly inhibits TGF-β1 production, we examined the effect of CC-401 on AngII–induced TGF-β1 secretion by the proximal tubular epithelial cell line HK-2. The addition of 1 μM AngII induced a two-fold increase in TGF-β1 secretion, which was suppressed in a dosage-dependent manner by CC-401, with a significant reduction observed with 4 μM CC-401 (Figure 10).

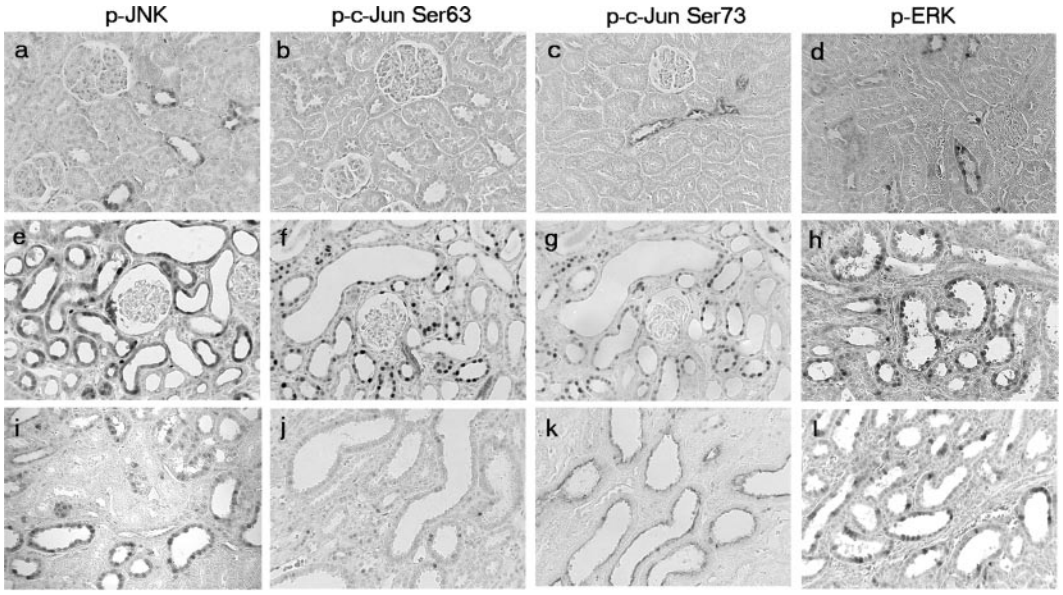

Figure 6. Detection of JNK and ERK activation by immunoperoxidase staining in rat UUO. Immunostaining of normal rat kidney detects staining for p-JNK in the cytoplasm and nucleus of collecting duct cells in the renal cortex (A); no signal for p-c-Jun Ser63 (B); luminal staining for p-c-Jun Ser73 in collecting ducts (C), and nuclear and cytoplasmic staining for p-ERK in collecting ducts (D). Immunostaining of day 7 UUO shows a marked increase in p-JNK with staining of cortical tubules, many of which show marked dilation, and some interstitial cells (E); nuclear staining for p-c-Jun Ser63 in many tubules, with a distribution similar to that for p-JNK (F); nuclear staining for p-c-Jun Ser73 in many tubules in a pattern very similar to that of p-c-Jun Ser63 (G); and nuclear staining for p-ERK in many tubules, including damaged tubules (H). Immunostaining of CC-401–treated day 7 UUO shows a partial reduction in p-JNK immunostaining compared with untreated UUO, but increased p-JNK staining is still evident in dilated tubules (I); an almost complete abrogation of p-c-Jun Ser63 staining (J); an almost complete abrogation of nuclear p-c-Jun Ser73 staining, although luminal staining is evident in damaged tubules (K); and no effect on the increase in p-ERK staining in the UUO kidney (L). Magnification, ×250.

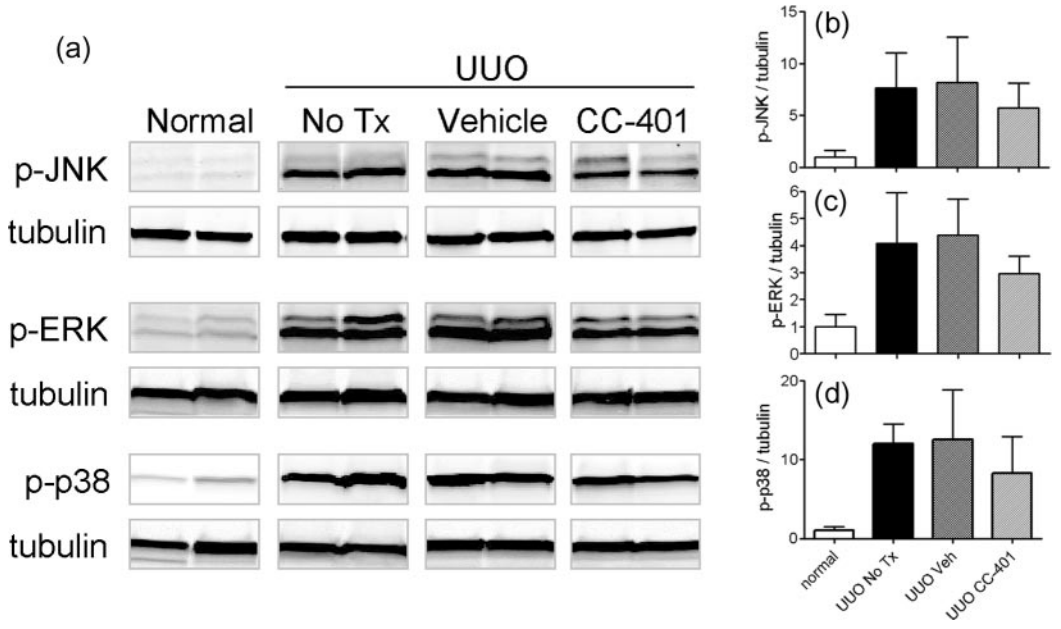

Figure 7. CC-401 does not affect phosphorylation of mitogen-activated protein kinases (MAPK) in rat UUO. (A) Western blotting of whole-kidney lysates shows increased phosphorylation of JNK, ERK, and p38 in rat UUO compared with normal kidney. No difference is seen with vehicle (Veh) or CC-401 treatment of UUO. Quantification of the ratio of phosphorylated MAPK to tubulin is shown for p-JNK (B), p-ERK (C), and p-p38 (D). For each individual MAPK, all UUO groups were increased significantly compared with normal kidney ($P < 0.05$), but no difference was seen between the various UUO groups. Data are means ± SD for groups of six rats with statistical analysis by ANOVA.

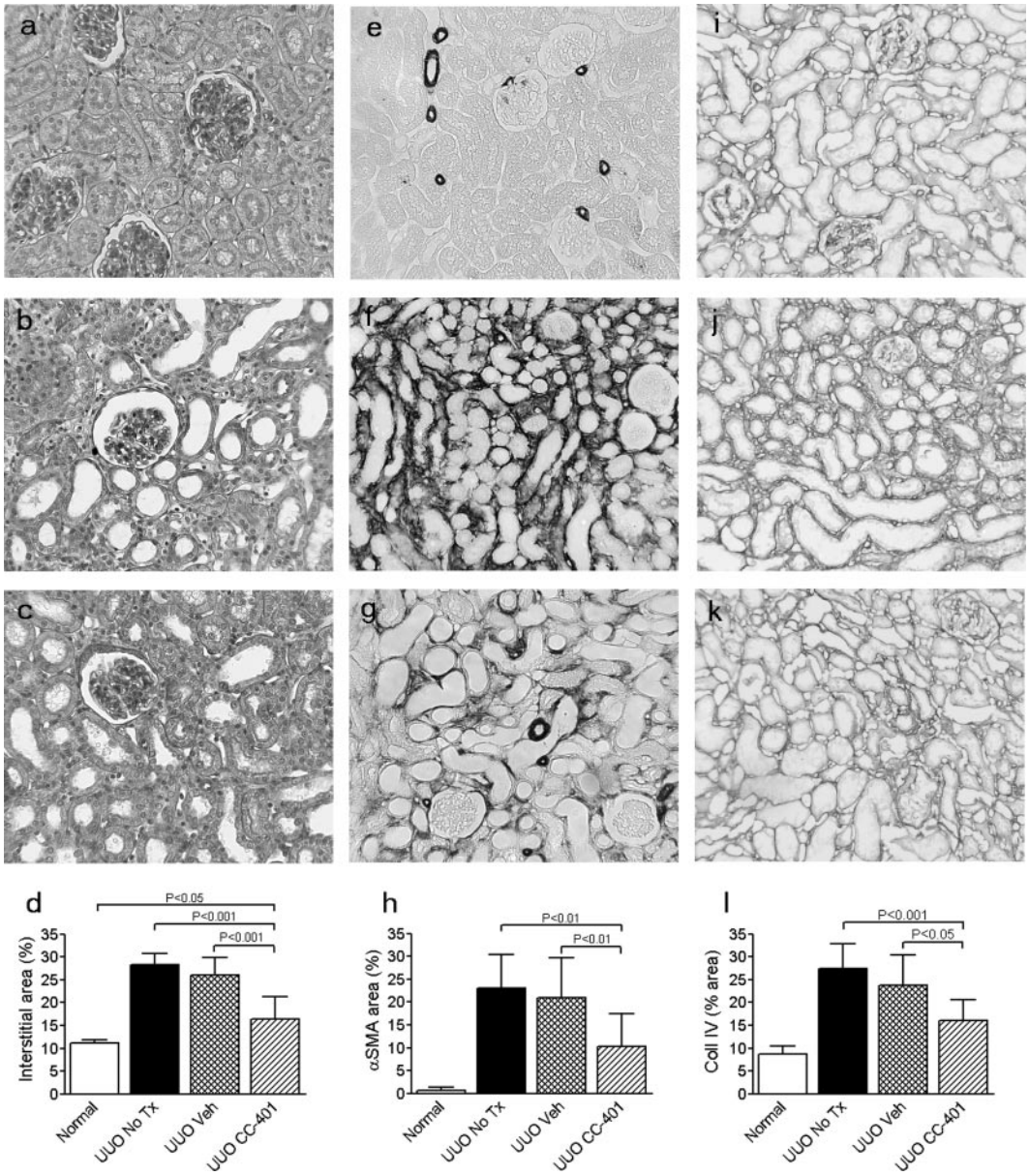

Figure 8. CC-401 suppresses renal fibrosis in rat UUO. Groups of rats underwent UUO surgery and received CC-401, vehicle (Veh), or no treatment (No Tx) and were killed 7 d later. Periodic acid-Schiff–stained sections show that compared with normal rat kidney (A), ureter obstruction in the No Tx group resulted in tubular dilation and atrophy with an increase in interstitial area (B). CC-401 treatment of UUO did not prevent tubular dilation, but it did suppress the increase in interstitial area. (D) Graph quantifying the interstitial area in all animal groups. Immunostaining for α-SMA identified arteries and arterioles in normal rat kidney (E), whereas in the untreated UUO group is a dramatic accumulation of interstitial α-SMA$^+$ myofibroblasts (F), which was reduced by CC-401 treatment (G). (H) Graph quantifying the area of interstitial α-SMA immunostaining in all animal groups. Immunostaining shows collagen IV in glomerular and tubular basement membranes in normal rat kidney (I). A marked increase in interstitial collagen IV is evident in untreated UUO (J), which was prevented in part by CC-401 treatment (K). (L) Graph quantifying the area of interstitial collagen IV immunostaining in all animal groups. Data are means $\pm$ SD for groups of 10 to 14 rats with statistical analysis by ANOVA. Magnifications: $\times$250 in A through C; $\times$160 in E through G and I through K.

Tubular epithelial cell apoptosis was evident in the obstructed kidney as assessed by immunostaining for cleaved caspase-3, and this was reduced by approximately 50% with CC-401 treatment (Figure 11A). Apoptosis of interstitial cells also was evident in the obstructed kidney. This was reduced by CC-401 treatment, but this failed to reach statistical significance (Figure 11B). A marked increase in the proliferation of interstitial and tubular cells was apparent in the obstructed kidney (Figure 11, C and D). Although CC-401 reduced the mean number of BrdU$^+$ proliferating interstitial cells, this did not

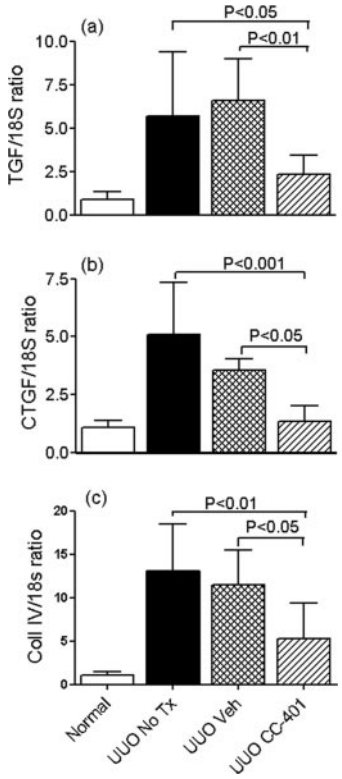

Figure 9. CC-401 suppresses the expression of profibrotic growth factors in rat UUO. Groups of rats underwent UUO surgery and received CC-401, vehicle (Veh), or no treatment (No Tx) and were killed 7 d later. Real-time reverse transcriptase–PCR was used to analyze renal levels of TGF-β1 (A), connective tissue growth factor (CTGF) (B), and collagen IV (C) mRNA relative to 18S rRNA. Data are means ± SD for groups of eight rats with statistical analysis by ANOVA.

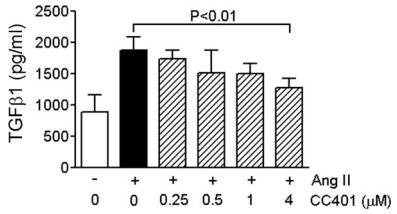

Figure 10. CC-401 inhibits angiotensin II (AngII)-induced TGF-β1 secretion *in vitro*. Stimulation of cultured HK-2 proximal tubules with 1 μM AngII for 48 h caused a two-fold increase TGF-β1 secretion ($P < 0.001$) as quantified by ELISA. CC-401 inhibited TGF-β1 secretion in a dosage-dependent manner. One experiment of three is shown, all of which showed similar results. Replicates of six were used in each condition, and results were analyzed by ANOVA.

reach statistical significance. Last, interstitial accumulation of ED1$^+$ macrophages in the obstructed kidney was not affected by CC-401 treatment (Figure 11E).

Discussion

This study examined the relative contribution of JNK1 and JNK2 isoforms to JNK signaling in normal or diseased kidney.

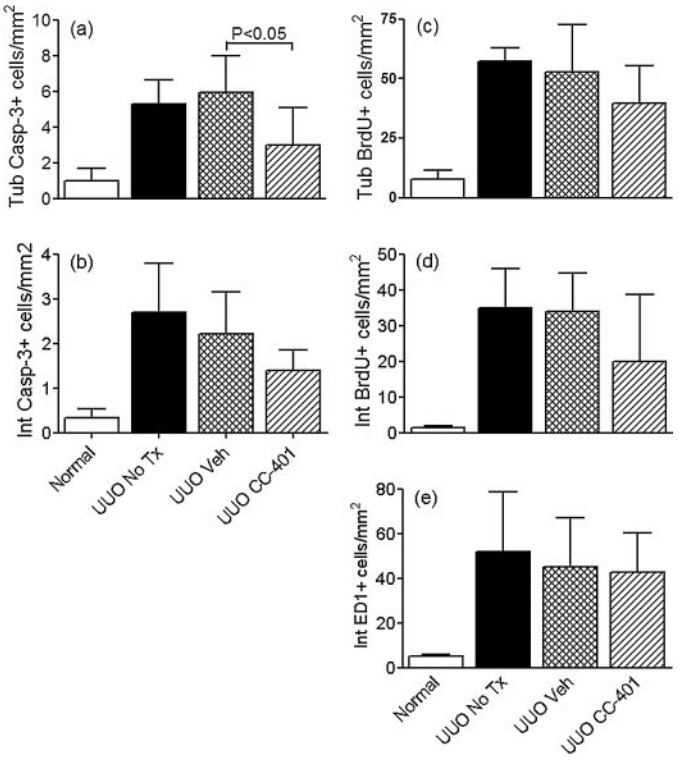

Figure 11. CC-401 suppresses tubular epithelial cell apoptosis in rat UUO. Groups of rats underwent UUO surgery and received CC-401, vehicle (Veh), or no treatment (No Tx) and were killed 7 d later. Tubular apoptosis (A) and interstitial cells apoptosis (B) were assessed by scoring cells that were stained for cleaved caspase-3. Proliferation of tubular epithelial cells (C) and interstitial cells (D) was assessed by immunostaining for BrdU incorporation. (E) Interstitial ED1$^+$ macrophages were assessed by immunostaining. Data are means ± SD for groups of 10 to 14 rats with statistical analysis by ANOVA.

We found substantial redundancy between JNK1 and JNK2 in regard to JNK signaling in both normal kidney and the obstructed kidney. Indeed, the distribution pattern of the marked increase in JNK phosphorylation and of p-c-Jun Ser63 and p-c-Jun Ser73 in the obstructed kidney was unaltered in *Jnk1−/−* and *Jnk2−/−* mice, although Western blotting did reveal a significant reduction in total JNK phosphorylation in the obstructed kidney in *Jnk1−/−* mice.

Phosphorylation of JNK was identified in collecting ducts and parietal epithelial cells in normal mouse and rat kidney. It is not clear whether JNK signaling in the normal kidney simply reflects osmotic or mechanical stress or plays an important physiologic function. A number of *in vitro* studies have demonstrated that mechanical and osmotic stresses can activate the JNK pathway (29–34). However, JNK activation does not seem to be critical for normal renal function because the use of CEP-1347, a drug that blocks several signaling pathways, including JNK, has been shown to be safe and well tolerated in short-term (35) and long-term clinical trials in Parkinson's disease (Clinical Trial NCT0004002).

This is the first study to examine JNK signaling in renal

fibrosis. For examination of this question, it is important to recognize that JNK signaling is involved in the innate and adaptive immune response that often is the cause of tissue injury to which fibrosis is the response. Therefore, to delineate the role of JNK signaling in the fibrotic response without the potential complication of modifying the immune response, we examined the UUO model in which fibrosis develops in response to a nonimmune, mechanical insult in a lymphocyte-independent manner (26).

Given the extensive redundancy between JNK1 and JNK2 isoforms, it was not surprising that neither *Jnk1−/−* nor *Jnk2−/−* mice were protected from the development of renal fibrosis in the UUO model. However, administration of CC-401, which inhibits all JNK isoforms, provided substantial protection from renal fibrosis in the rat model on the basis of reduced collagen IV deposition and α-SMA$^+$ myofibroblast accumulation. Fibrosis in the UUO is model depends on the profibrotic growth factors TGF-β1 and CTGF (23–25), common mechanisms that drive fibrosis in other forms of kidney disease. Upregulation of TGF-β1 in the UUO model depends on AngII (36). We found that CC-401 inhibited AngII-induced TGF-β1 secretion by cultured tubular epithelial cells in a dosage-dependent manner, showing a significant effect in the concentration range that was achieved *in vivo*. These results are consistent with previous *in vitro* studies that demonstrated that AngII-induced TGF-β production in mesangial cells operates in JNK-dependent manner (37). Therefore, the reduction in TGF-β1 mRNA levels probably is a major mechanism by which CC-401 treatment suppresses renal fibrosis in the UUO model. The identification of an activating protein-1 (AP-1) binding site in the TGF-β gene promoter provides a mechanism whereby JNK blockade can inhibit TGF-β gene transcription directly (38). The reduction in collagen IV mRNA levels is consistent with a reduction in TGF-β1 activity. Of note, JNK activation was identified in both tubular epithelial cells and interstitial α-SMA$^+$ myofibroblasts in the obstructed kidney—the two cell types that were identified as being responsible for the increase in renal TGF-β1 mRNA levels in this model (36,39,40). CC-401 treatment also prevented an increase in CTGF gene transcription in the obstructed kidney. This probably reflects an indirect effect of the reduction in TGF-β1 mRNA levels. However, CC-401 may have inhibited the CTGF response in a direct manner because TGF-β1–induced CTGF production in human lung fibroblasts is JNK dependent (19).

The reduction in α-SMA$^+$ myofibroblast accumulation that was seen with CC-401 treatment in the UUO model could operate *via* indirect or direct mechanisms. The reduction in TGF-β1 production that was seen with CC-401 treatment may be an indirect mechanism to reduce α-SMA$^+$ myofibroblast accumulation because TGF-β1 is associated with the migration of fibrocytes from the circulation into sites of tissue injury (41), TGF-β1 can induce the differentiation of local fibroblasts into α-SMA$^+$ myofibroblasts (42), and TGF-β1 can promote the transition of tubular epithelial cells into α-SMA$^+$ myofibroblasts (43,44). Local proliferation also contributes to interstitial myofibroblast accumulation in the obstructed kidney. *In vitro* studies that used antisense oligonucleotides implicated JNK2 in promoting proliferation of murine fibroblasts (45). CC-401 treatment reduced interstitial cell proliferation in rat UUO, but this failed to reach statistical significance, whereas interstitial cell proliferation was unaltered in *Jnk1−/−* or *Jnk2−/−* UUO, indicating that JNK signaling does not promote renal fibroblast or myofibroblast proliferation *in vivo*.

A direct link between JNK activation and tubular epithelial cell apoptosis was identified by immunostaining of serial sections for cleaved caspase-3 and p-c-Jun Ser63. However, most apoptotic cells did not exhibit JNK signaling, indicating either that the c-Jun protein had been de-phosphorylated/degraded before activation of caspase-3 or that other pathways contribute to apoptosis in this model. Tubular cell apoptosis was suppressed by JNK blockade with CC-401. Furthermore, studies in mouse UUO showed a nonredundant role for JNK1 but not JNK2 in the apoptosis of tubular epithelial cells and interstitial cells. This is the first *in vivo* study to demonstrate that renal cell apoptosis depends, at least in part, on the JNK signaling pathway. The role of individual JNK forms in apoptotic cell death are cell type dependent. Both *Jnk1* and *Jnk2* gene–deficient mice have reduced apoptosis of myocytes after cardiac ischemia/reperfusion injury (46); however, JNK1 but not JNK2 is involved in TNF-α–induced apoptosis of fibroblasts (47). These data also are consistent with studies in liver ischemia/reperfusion injury in which CC-401 treatment reduced hepatocyte apoptosis and improved liver function (11,12).

The finding that JNK signaling plays a critical role in tubular epithelial cell apoptosis in the obstructed kidney confirms previous *in vitro* studies that showed that oxidative stress–induced tubular cell apoptosis is mediated in part through JNK signaling (48,49). Similarly, stretch-induced apoptosis of cultured tubular epithelial cells also depends, in part, on JNK signaling (50). Macrophages also have been postulated as mediators of tubular epithelial cell apoptosis (51). CC-401 treatment had no effect on interstitial macrophage accumulation in the obstructed kidney; however, we cannot rule out that JNK signaling may have a role in macrophage activation that leads to tubular epithelial cell apoptosis in the UUO model, because previous adoptive transfer studies in rat anti–glomerular basement membrane disease have shown that blockade of JNK signaling in macrophages can reduce substantially macrophage-mediated renal injury without any effect on macrophage recruitment into the injured kidney (52).

JNK blockade using CC-401 did not completely abrogate renal fibrosis in the obstructed rat kidney, suggesting that other pathways contribute to the pathogenesis of interstitial fibrosis. The closely related pathway p38 mitogen activated protein kinase has been shown to promote renal fibrosis in the UUO model (53). It is interesting that p38 blockade caused a partial reduction in interstitial α-SMA$^+$ myofibroblast accumulation and collagen IV deposition without affecting the upregulation of TGF-β1 mRNA levels (53). The distinct differences between JNK and p38 signaling pathways in regard to transcription of the TGF-β1 gene raises the question as to whether combined inhibition of JNK and p38 pathways could provide an additive benefit in suppressing renal fibrosis in this model.

The specificity of CC-401 for the JNK pathway was examined

in several ways in this study. First, phosphorylation of c-Jun at Ser63 and Ser73 was blocked efficiently by CC-401. Although the specificity of this reaction has been questioned (54), several studies have argued strongly that ERK is unable to phosphorylate the amino terminus of c-Jun (3–6). Furthermore, blockade of ERK signaling in the mouse UUO model using the MEK1 inhibitor UO126 failed to prevent the phosphorylation of c-Jun at Ser63 or Ser73 (Y.H. and D.J.N.-P., unpublished data). Second, the peak serum level of CC-401 was in the target range of 0.5 to 2.0 μM, at which CC-401 has at least 40-fold selectivity for JNK compared with a panel of related kinases. Third, CC-401 treatment had no effect on phosphorylation of ERK or p38 kinases in the UUO model or in cell culture studies. However, in studies of this type, it is impossible to exclude the possibility that the drug being examined exerts effects on some unidentified pathway.

Conclusion

This is the first study to demonstrate that JNK signaling plays a pathogenic role in renal fibrosis and tubular apoptosis. Whereas the JNK1 and JNK2 isoforms showed redundancy with respect to the development of renal fibrosis in the obstructed kidney, JNK1 was identified to play a nonredundant role in tubular cell apoptosis. These studies identify the JNK pathway as a potential therapeutic target in progressive kidney disease.

Acknowledgments

This study was funded by the National Health and Medical Research Council (NHMRC) of Australia and by Celgene. We acknowledge a NHMRC Scholarship (R.F.), a NHMRC/Kidney Health Australia/Australian and New Zealand Society of Nephrology Career Development Award (G.T.), and a NHMRC Senior Research Fellowship (D.N.-P.).

Part of these studies were presented at the 38th annual meeting of the American Society of Nephrology; November 8 through 13, 2005; Philadelphia, PA.

Disclosures

Celgene in part funded these studies, and D.N.-P. acts as a consultant for Celgene.

References

1. Manning AM, Davis RJ: Targeting JNK for therapeutic benefit: From junk to gold? *Nat Rev Drug Discov* 2: 554–565, 2003
2. Bogoyevitch MA, Boehm I, Oakley A, Ketterman AJ, Barr RK: Targeting the JNK MAPK cascade for inhibition: Basic science and therapeutic potential. *Biochim Biophys Acta* 1697: 89–101, 2004
3. Pulverer BJ, Kyriakis JM, Avruch J, Nikolakaki E, Woodgett JR: Phosphorylation of c-jun mediated by MAP kinases. *Nature* 353: 670–674, 1991
4. Minden A, Lin A, Smeal T, Derijard B, Cobb M, Davis R, Karin M: c-Jun N-terminal phosphorylation correlates with activation of the JNK subgroup but not the ERK subgroup of mitogen-activated protein kinases. *Mol Cell Biol* 14: 6683–6688, 1994
5. Vinciguerra M, Vivacqua A, Fasanella G, Gallo A, Cuozzo C, Morano A, Maggiolini M, Musti AM: Differential phosphorylation of c-Jun and JunD in response to the epidermal growth factor is determined by the structure of MAPK targeting sequences. *J Biol Chem* 279: 9634–9641, 2004
6. Wang YN, Chen YJ, Chang WC: Activation of extracellular signal-regulated kinase signaling by epidermal growth factor mediates c-Jun activation and p300 recruitment in keratin 16 gene expression. *Mol Pharmacol* 69: 85–98, 2006
7. Deng Y, Ren X, Yang L, Lin Y, Wu X: A JNK-dependent pathway is required for TNFalpha-induced apoptosis. *Cell* 115: 61–70, 2003
8. Yu C, Minemoto Y, Zhang J, Liu J, Tang F, Bui TN, Xiang J, Lin A: JNK suppresses apoptosis via phosphorylation of the proapoptotic Bcl-2 family protein BAD. *Mol Cell* 13: 329–340, 2004
9. Liu J, Lin A: Role of JNK activation in apoptosis: A double-edged sword. *Cell Res* 15: 36–42, 2005
10. Yang DD, Kuan CY, Whitmarsh AJ, Rincon M, Zheng TS, Davis RJ, Rakic P, Flavell RA: Absence of excitotoxicity-induced apoptosis in the hippocampus of mice lacking the Jnk3 gene. *Nature* 389: 865–870, 1997
11. Uehara T, Bennett B, Sakata ST, Satoh Y, Bilter GK, Westwick JK, Brenner DA: JNK mediates hepatic ischemia reperfusion injury. *J Hepatol* 42: 850–859, 2005
12. Uehara T, Xi Peng X, Bennett B, Satoh Y, Friedman G, Currin R, Brenner DA, Lemasters J: c-Jun N-terminal kinase mediates hepatic injury after rat liver transplantation. *Transplantation* 78: 324–332, 2004
13. Chan ED, Riches DW: IFN-gamma + LPS induction of iNOS is modulated by ERK, JNK/SAPK, and p38(mapk) in a mouse macrophage cell line. *Am J Physiol Cell Physiol* 280: C441–C450, 2001
14. Han Z, Boyle DL, Chang L, Bennett B, Karin M, Yang L, Manning AM, Firestein GS: c-Jun N-terminal kinase is required for metalloproteinase expression and joint destruction in inflammatory arthritis. *J Clin Invest* 108: 73–81, 2001
15. Dong C, Yang DD, Wysk M, Whitmarsh AJ, Davis RJ, Flavell RA: Defective T cell differentiation in the absence of Jnk1. *Science* 282: 2092–2095, 1998
16. Dong C, Yang DD, Tournier C, Whitmarsh AJ, Xu J, Davis RJ, Flavell RA: JNK is required for effector T-cell function but not for T-cell activation. *Nature* 405: 91–94, 2000
17. Yang DD, Conze D, Whitmarsh AJ, Barrett T, Davis RJ, Rincon M, Flavell RA: Differentiation of CD4+ T cells to Th1 cells requires MAP kinase JNK2. *Immunity* 9: 575–585, 1998
18. Hocevar BA, Brown TL, Howe PH: TGF-beta induces fibronectin synthesis through a c-Jun N-terminal kinase-dependent, Smad4-independent pathway. *EMBO J* 18: 1345–1356, 1999
19. Utsugi M, Dobashi K, Ishizuka T, Masubuchi K, Shimizu Y, Nakazawa T, Mori M: C-Jun-NH2-terminal kinase mediates expression of connective tissue growth factor induced by transforming growth factor-beta1 in human lung fibroblasts. *Am J Respir Cell Mol Biol* 28: 754–761, 2003
20. Peng H, Takano T, Papillon J, Bijian K, Khadir A, Cybulsky AV: Complement activates the c-Jun N-terminal kinase/stress-activated protein kinase in glomerular epithelial cells. *J Immunol* 169: 2594–2601, 2002
21. Yang CW, Ahn HJ, Jung JY, Kim WY, Li C, Choi BS, Kim HW, Kim YS, Moon IS, Kim J, Bang BK: Preconditioning

with cyclosporine A or FK506 differentially regulates mitogen-activated protein kinase expression in rat kidneys with ischemia/reperfusion injury. *Transplantation* 75: 20–24, 2003
22. Fujita H, Omori S, Ishikura K, Hida M, Awazu M: ERK and p38 mediate high-glucose-induced hypertrophy and TGF-beta expression in renal tubular cells. *Am J Physiol Renal Physiol* 286: F120–F126, 2004
23. Yokoi H, Mukoyama M, Nagae T, Mori K, Suganami T, Sawai K, Yoshioka T, Koshikawa M, Nishida T, Takigawa M, Sugawara A, Nakao K: Reduction in connective tissue growth factor by antisense treatment ameliorates renal tubulointerstitial fibrosis. *J Am Soc Nephrol* 15: 1430–1440, 2004
24. Miyajima A, Chen J, Lawrence C, Ledbetter S, Soslow RA, Stern J, Jha S, Pigato J, Lemer ML, Poppas DP, Vaughan ED, Felsen D: Antibody to transforming growth factor-beta ameliorates tubular apoptosis in unilateral ureteral obstruction. *Kidney Int* 58: 2301–2313, 2000
25. Isaka Y, Tsujie M, Ando Y, Nakamura H, Kaneda Y, Imai E, Hori M: Transforming growth factor-beta 1 antisense oligodeoxynucleotides block interstitial fibrosis in unilateral ureteral obstruction. *Kidney Int* 58: 1885–1892, 2000
26. Shappell SB, Gurpinar T, Lechago J, Suki WN, Truong LD: Chronic obstructive uropathy in severe combined immunodeficient (SCID) mice: Lymphocyte infiltration is not required for progressive tubulointerstitial injury. *J Am Soc Nephrol* 9: 1008–1017, 1998
27. Masaki T, Foti R, Hill PA, Ikezumi Y, Atkins RC, Nikolic-Paterson DJ: Activation of the ERK pathway precedes tubular proliferation in the obstructed rat kidney. *Kidney Int* 63: 1256–1264, 2003
28. Pillebout E, Weitzman JB, Burtin M, Martino C, Federici P, Yaniv M, Friedlander G, Terzi F: JunD protects against chronic kidney disease by regulating paracrine mitogens. *J Clin Invest* 112: 843–852, 2003
29. Engel ME, McDonnell MA, Law BK, Moses HL: Interdependent SMAD and JNK signaling in transforming growth factor-beta-mediated transcription. *J Biol Chem* 274: 37413–37420, 1999
30. Huang Z, Tunnacliffe A: Response of human cells to desiccation: Comparison with hyperosmotic stress response. *J Physiol* 558: 181–191, 2004
31. Ingram AJ, Ly H, Thai K, Kang M, Scholey JW: Activation of mesangial cell signaling cascades in response to mechanical strain. *Kidney Int* 55: 476–485, 1999
32. Koh YH, Che W, Higashiyama S, Takahashi M, Miyamoto Y, Suzuki K, Taniguchi N: Osmotic stress induces HB-EGF gene expression via Ca(2+)/Pyk2/JNK signal cascades in rat aortic smooth muscle cells. *J Biochem (Tokyo)* 130: 351–358, 2001
33. Malek AM, Goss GG, Jiang L, Izumo S, Alper SL: Mannitol at clinical concentrations activates multiple signaling pathways and induces apoptosis in endothelial cells. *Stroke* 29: 2631–2640, 1998
34. Martineau LC, Gardiner PF: Insight into skeletal muscle mechanotransduction: MAPK activation is quantitatively related to tension. *J Appl Physiol* 91: 693–702, 2001
35. Jennings D, Stavris K, Counihan T, Gardiner I, Factor S, Evans S, Feigin A, Shannon B, Fernandez H: The safety and tolerability of a mixed lineage kinase inhibitor (CEP-1347) in PD. *Neurology* 62: 330–332, 2004
36. Kaneto H, Morrissey J, Klahr S: Increased expression of TGF-beta 1 mRNA in the obstructed kidney of rats with unilateral ureteral ligation. *Kidney Int* 44: 313–321, 1993
37. Naito T, Masaki T, Nikolic-Paterson DJ, Tanji C, Yorioka N, Kohno N: Angiotensin II induces thrombospondin-1 production in human mesangial cells via p38 MAPK and JNK: A mechanism for activation of latent TGF-beta1. *Am J Physiol Renal Physiol* 286: F278–F287, 2004
38. Wu Z, Zhou Q, Lan Y, Wang Y, Xu X, Jin H: AP-1 complexes mediate oxidized LDL-induced overproduction of TGF-beta(1) in rat mesangial cells. *Cell Biochem Funct* 22: 237–247, 2004
39. Fukuda K, Yoshitomi K, Yanagida T, Tokumoto M, Hirakata H: Quantification of TGF-beta1 mRNA along rat nephron in obstructive nephropathy. *Am J Physiol Renal Physiol* 281: F513–F521, 2001
40. Le Meur Y, Tesch GH, Hill PA, Mu W, Foti R, Nikolic-Paterson DJ, Atkins RC: Macrophage accumulation at a site of renal inflammation is dependent on the M-CSF/c-fms pathway. *J Leukoc Biol* 72: 530–537, 2002
41. Yang L, Scott PG, Giuffre J, Shankowsky HA, Ghahary A, Tredget EE: Peripheral blood fibrocytes from burn patients: Identification and quantification of fibrocytes in adherent cells cultured from peripheral blood mononuclear cells. *Lab Invest* 82: 1183–1192, 2002
42. Evans RA, Tian YC, Steadman R, Phillips AO: TGF-beta1-mediated fibroblast-myofibroblast terminal differentiation-the role of Smad proteins. *Exp Cell Res* 282: 90–100, 2003
43. Fan JM, Ng YY, Hill PA, Nikolic-Paterson DJ, Mu W, Atkins RC, Lan HY: Transforming growth factor-beta regulates tubular epithelial-myofibroblast transdifferentiation in vitro. *Kidney Int* 56: 1455–1467, 1999
44. Iwano M, Neilson EG: Mechanisms of tubulointerstitial fibrosis. *Curr Opin Nephrol Hypertens* 13: 279–284, 2004
45. Du L, Lyle CS, Hall-Obey TB, Gaarde WA, Muir JA, Bennett BL, Chambers TC: Inhibition of cell proliferation and cell cycle progression by specific inhibition of basal JNK activity: Evidence that mitotic Bcl-2 phosphorylation is JNK-independent. *J Biol Chem* 279: 11957–11966, 2004
46. Kaiser RA, Liang Q, Bueno OF, Huang Y, Lackey T, Klevitsky R, Hewett TE, Molkentin JD: Genetic inhibition or activation of JNK1/2 each protect the myocardium from ischemia-reperfusion-induced cell death in vivo. *J Biol Chem* 280: 32602–32608, 2005
47. Liu J, Minemoto Y, Lin A: c-Jun N-terminal protein kinase 1 (JNK1), but not JNK2, is essential for tumor necrosis factor alpha-induced c-Jun kinase activation and apoptosis. *Mol Cell Biol* 24: 10844–10856, 2004
48. Pat BK, Cuttle L, Watters D, Yang T, Johnson DW, Gobe GC: Fibrogenic stresses activate different mitogen-activated protein kinase pathways in renal epithelial, endothelial or fibroblast cell populations. *Nephrology (Carlton)* 8: 196–204, 2003
49. Arany I, Megyesi JK, Kaneto H, Tanaka S, Safirstein RL: Activation of ERK or inhibition of JNK ameliorates H2O2 cytotoxicity in mouse renal proximal tubule cells. *Kidney Int* 65: 1231–1239, 2004
50. Nguyen HT, Hsieh MH, Gaborro A, Tinloy B, Phillips C, Adam RM: JNK/SAPK and p38 SAPK-2 mediate mechanical stretch-induced apoptosis via caspase-3 and -9 in NRK-52E renal epithelial cells. *Nephron Exp Nephrol* 102: e49–e61, 2006

51. Lange-Sperandio B, Fulda S, Vandewalle A, Chevalier RL: Macrophages induce apoptosis in proximal tubule cells. *Pediatr Nephrol* 18: 335–341, 2003
52. Ikezumi Y, Hurst L, Atkins RC, Nikolic-Paterson DJ: Macrophage-mediated renal injury is dependent on signaling via the JNK pathway. *J Am Soc Nephrol* 15: 1775–1784, 2004
53. Stambe C, Atkins RC, Tesch GH, Masaki T, Schreiner GF, Nikolic-Paterson DJ: The role of p38alpha mitogen-activated protein kinase activation in renal fibrosis. *J Am Soc Nephrol* 15: 370–379, 2004
54. Morton S, Davis RJ, McLaren A, Cohen P: A reinvestigation of the multisite phosphorylation of the transcription factor c-Jun. *EMBO J* 22: 3876–3886, 2003